Nisar et al. | J Pure Appl Microbiol | 14(3):1789-1800 | September 2020
Article 6605 | https://doi.org/10.22207/JPAM.14.3.17

Print ISSN: 0973-7510; E-ISSN: 2581-690X

RESEARCH ARTICLE OPEN ACCESS

Synthesis, Characterization, and Antimicrobial Properties of Sparfloxacin-Mediated Noble Metal Nanoparticles

Muhammad Nisar[1], Shujaat Ali Khan[2], Maryam Gul[2], Abdur Rauf[3], Salman Zafar[2] and Mohamed Fawzy Ramadan[4,5]*

[1]Office of Research, Innovation and Commercialization, University of Peshawar, Peshawar - 25120, Pakistan.
[2]Institute of Chemical Sciences, University of Peshawar, Peshawar - 25120, Pakistan.
[3]Department of Chemistry, University of Swabi, Swabi, Anbar - 23561, KPK, Pakistan.
[4]Deanship of Scientific Research, Umm Al-Qura University, Makkah, P.O.Box 715, Saudi Arabia.
[5]Biochemistry Department, Faculty of Agriculture, Zagazig University, Zagazig - 44519, Zagazig, Egypt.

Abstract

The aim of the current research finding was to synthesize, characterize and antibacterial evaluation of sparfloxacin-mediated noble metal nanoparticles. Noble metal [silver (Ag), and gold (Au)] nanoparticles (NPs), mediated with fluoroquinolone, an anti-bacterial drug [Sparfloxacin, (Sp)], was synthesized by a facile and convenient procedure. Formulated Ag-Sp NPs, and Au-Sp NPs exhibited stability against variation in pH, NaCl solution, temperature, and time. The structural topographies of Ag-Sp, and Au-Sp NPs were determined by fourier transform infrared spectroscopy (FTIR), UV-visible spectroscopy (UV-Vis), scanning electron microscopy (SEM) atomic force microscopy (AFM), and energy dispersive X-ray (EDX). UV-Vis revealed the formulation of NPs by showing typical surface Plasmon absorption maxima at 410 nm for Ag-Sp NPs and 555 nm for Au-Sp NPs. The AFM and SEM analysis ascertained stable mono dispersed Ag-Sp NPs and Au-Sp NPs in the size range of 40-50 nm, and 70-80 nm, respectively. Ag-Sp, and Au-Sp NPs exhibited antibacterial traits against *Bacillus subtilis*, *Staphylococcus aureus*, and *Klebsiella pneumonia*, showing a zone of inhibition (ZOI) ranging from 20±0·98 mm to 24±0·94 mm (Ag-Sp NPs), and 22±0·79 mm to 26±0·92 mm (Au-Sp NPs) at dose of 3 mg/mL.

Keywords: Sparfloxacin, Silver, Gold, UV-VIS spectroscopy, FTIR, AFM, SEM, Anti-bacterial activity

***Correspondence:** mhassanien@uqu.edu.sa

(Received: August 22, 2020; accepted: September 16, 2020)

Citation: Nisar M, Khan SA, Gul M, Rauf A, Zafar S, Ramadan MF. Synthesis, Characterization, and Antimicrobial Properties of Sparfloxacin-Mediated Noble Metal Nanoparticles. *J Pure Appl Microbiol.* 2020;14(3):1789-1800. doi: 10.22207/JPAM.14.3.17

INTRODUCTION

Nanosciences have attained great interest due to the syntheses of metal nanoparticles (NPs). Several noble nanomaterials such as silver, gold, mercury, platinum, copper and zinc are employed in the biological, agricultural and biomedical fields (Arvizo et al. 2012; Johnson alias Antonysamy et al., 2017). Ag NPs have been well-known in man-made activities since ancient time (Mikhailov et al., 2019). The crystalline nature and morphology of NPs play pivotal role in the parameter of their chemical and physical traits (Coe et al., 2002; Mittal et al., 2016; Rizwan et al., 2020). NPs are the building blocks of nanotechnology that shows novel optical and biological properties when compared with the bulk material (Keshavamurthy, Srinath, and Ravishankar Rai, 2017). NPs are highly exploited owing to their unique traits such as drug delivery, antimicrobial, electrical, and catalytic properties (Cuenya 2010; Saravanan, Vemu, and Barik 2011; Mittal et al., 2016).

Noble metal NPs synthesis has utmost importance (Alvarez, 1997; Reed and Lee, 2003; Cao, 2004; Wang et l., 2005; Nath et al., 2008). Synthesis of noble metal NPs has gained much attention because of their optical, magnetic, electronic, and catalytic properties, that depend on their shape and size (Reed and Lee, 2003; Cao, 2004). Furthermore, noble metal NPs exhibited surface plasmon resonance (SPR) in the infrared range as well as in the visible range, which is due to the oscillation of free electrons of the NPs in resonance with the frequency of the light wave, interacting with the noble metal NPs. SPR peak is the preliminary clue of noble metal NPs synthesis. In the synthesis of noble metal NPs, it is important to control particle size, shape and morphology (You et al., 2012).

Recently, gold nanoparticles (Au-NPs) became the subject of research interest due to their wide applications in biotechnology, biomedical, catalysis, drug delivery approaches, and electronics (Majumdar, Bag, and Ghosh, 2015). Because of their large surface to volume ratio, Au-NPs exhibit specific physicochemical traits, which make them attractive to be utilized in biomedical industry (Abdelghany et al, 2017). Au-NPs have advantages in biomedical applications over other NPs due to their non-cytotoxicity and biocompatibility (Xiangqian et al., 2011; Keshavamurthy, Srinath, and Ravishankar Rai, 2017). On the other hand, fabrication of silver nanoparticles (Ag-NPs) using *Schizophyllum radiatum* HE 863742.1 (Metuku et al., 2014), extracts of *Argemone mexicana* (Singh et al., 2011), *Crataegus douglasii* (Ghaffari-Moghaddam and Hadi-Dabanlou, 2014), Chick pea (Singh et al., 2013), *Ananas comosus* (Hyllested et al., 2015) and leaf extract of *Artemisia annua* (Basavegowda et al., 2014) have been reported (Mittal et al., 2016). The lignin capped Ag NPs was synthesized in water using a carbohydrate based polymer lignin as the stabilizing and reducing agents (Marulasiddeshwara et al., 2017). A facile, an environmental-friendly and a cheap procedure to biosynthesize of zinc oxide NPs (ZnO NPs) using the leaf extracts of *Berberis aristata* was also reported (Chandra et al., 2019).

The conjugates of noble metal NPs with antibodies and antibiotics were employed for selective photo-thermal killing of bacteria and protozoa (Rao et al., 2000; Pissuwan et al., 2007; Huang et al., 2007). The biosynthesized Ag NPs exhibited significant antimicrobial activity against various multi-drug resistant pathogens, which is comparable with standard antibiotic drug streptomycin (Maniraj et al., 2019) Being in practice for more than decades, quinolones form a group of potent antimicrobial agents (Mitscher, 2005; Zharov et al., 2010). Today, they are regarded as the most successful synthetic antimicrobial drugs (Andriole, 2000; Hooper and Rubinstein, 2003; Nath et al., 2008), which successfully inhibit the bacterial DNA replication (King et al., 2000; Turel, 2002). The third-generation quinolones including sparfloxacin, gatifloxacin, levofloxacin, and moxifloxacin exhibited a wide spectrum of activities against typical pathogens as well as Gram-negative bacteria, and Gram-positive bacteria (Stein, 1996).

Ag NPs have promising antibacterial properties against Gram positive and Gram negative bacterial strains (Ismail et al., 2018). Similarly the Ag NPs prepared from *Catharanthus roseus* leaf has been documented for wound healing with antioxidant and antimicrobial activity (Al-Shmgani et al., 2017). Ag NPs synthesized from *Aspergillus flavus* have been reported for cytotoxicity, and showed antioxidant, antimicrobial activity (Sulaiman et al., 2014; Sulaiman et al.,

2015). The prepared silver and gold NPs possess cytotoxicity, antioxidant, antimicrobial, anticancer, anti-inflammatory and phagocytic activities (Taha et al., 2019; Suliman et al., 2020; Waheeb et al., 2020).

It is the cry of the day to develop protocols for fabrication of noble metal NPs. Present study deals with the facile synthesis, and characteristics of sparfloxacin-mediated Ag-Sp/Au-Sp NPs (Scheme 1). The synthesized Ag-Sp/Au-Sp NPs were characterized using FTIR, UV-Vis, AFM and SEM. For the first time, the anti-bacterial activity of sparfloxacin-mediated Ag-Sp and Au-Sp NPs is reported.

MATERIALS AND METHODS

Materials

Silver nitrate (AgNO3) was procured from Sigma (St. Louis, MO, USA). Chlorauric acid (HAuCl4.3H2O), NaOH, NaCl, CH3OH and HCl were obtained from Merck (MA, USA). Sodium borohydride (NaBH4) was attained from Wako Pure Chem. Ind. Ltd. Sparfloxacin was obtained by Fozan Pharma Industries (pvt) Ltd. (Peshawar, Pakistan). Glassware were cleaned with aqua regia, washed with triply distilled water, and dried. All the solutions were freshly prepared using deionized-water and kept in dark. De-ionized water was used throughout the reactions for the Ag-Sp/Au-Sp NPs synthesis.

Synthesis of sparfloxacin-mediated silver and gold NPs (Ag-Sp and Au-Sp NPs)

The fresh stock solutions were prepared by using de-ionized water, (1 mM solutions of silver nitrate, tetrachloro auric acid, and sparfloxacin). Sparfloxacin drug (Fig. 1) is sparingly soluble in de-ionized water; hence methanol was used as co-solvent for preparation of drug solution. Ag-Sp and Au-Sp NPs were synthesized using NaBH4 as a mild chemical reductant. Reactions were carried out by mixing different volumes of sparfloxacin and metal salt solutions. The reaction mixtures were stirred robustly for 40 min at ambient temperature, followed by the drop wise addition of 0.2 mL of 50 mM NaBH4 solution. Gradual change

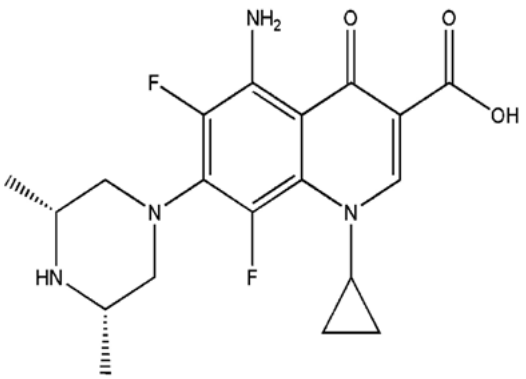

Fig. 1. Chemical structure of sparfloxacin

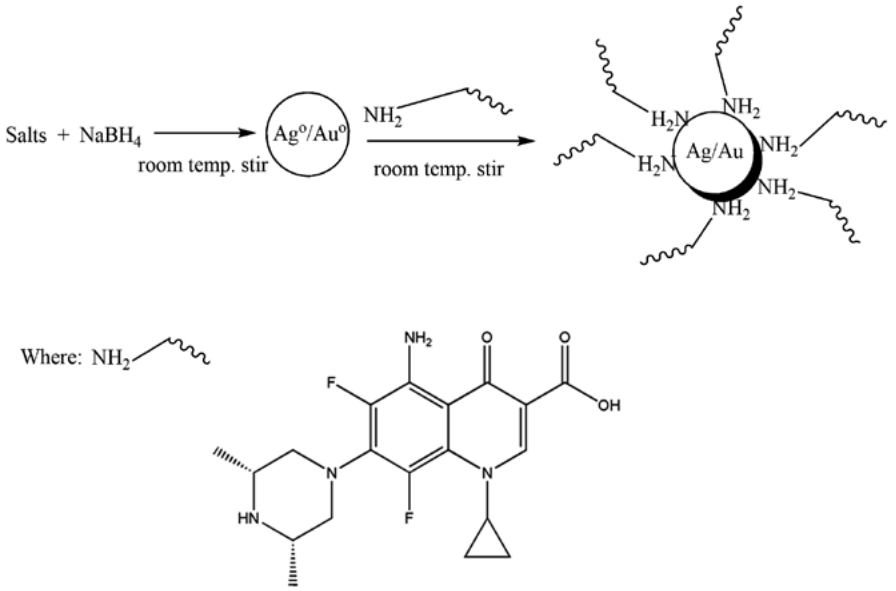

Scheme 1. Capping action of sparfloxacin with silver and gold NPs

in the solution color is a preliminary indication for the formation of Ag-Sp and Au-Sp NPs. After the addition of reducing agent, the light-yellow solution turned maroon, followed by brown and/ or ruby red, depend on the molar ratio of the metal to the drug (Fig.s 2 a & b). Absorption maxima of noble metal nanoparticles were recorded as a function of retention time in the range of 300 to 700 nm. For Ag-Sp NPs, the best optimal metal: drug ratio observed was 10:1, while for Au-Sp NPs the optimized ratio was 1:2 (metal: drug), at room temperature (Fig.s 2 a & b). The residual salts and drug were removed via centrifugation at 10 rpm. The supernatant, containing Ag-Sp or Au-Sp NPs was lyophilized and furthermore, subjected for characterization and biological evaluation.

Characterization of Ag-Sp and Au-Sp NPs

The synthesis of Ag-Sp and Au-Sp NPs were confirmed by atomic force microscopy (AFM), UV-Vis spectroscopy, fourier transform infrared spectroscopy (FTIR), scanning electron microscopy (SEM), and energy dispersive X-ray (EDX) techniques.

UV-VIS spectroscopy

Initial confirmation of the Ag-Sp and Au-Sp NPs synthesis was conducted using UV-VIS spectroscopy. UV-Vis spectra of Ag-Sp and Au-Sp NPs were screened using a Shimadzu UV-240, Hitachi U-3200 spectrophotometer.

FTIR analysis

FTIR was performed to detect functional groups and reducing agent using FTIR spectrometer. FTIR spectra were logged with a Shimadzu IR-460 spectrophotometer. For these measurements, Ag-Sp and Au-Sp NPs were lyophilized and small amount of freeze-dried sample (0.01 g Ag-Sp and Au-Sp NPs) were mixed with KBr to prepare round pellets for FTIR measurement.

AFM analysis

The shapes and sizes of Ag-Sp and Au-Sp NPs were analyzed using AFM (Multimode, NanoscopeIIIa, Veeco, CA, USA), in tapping mode.

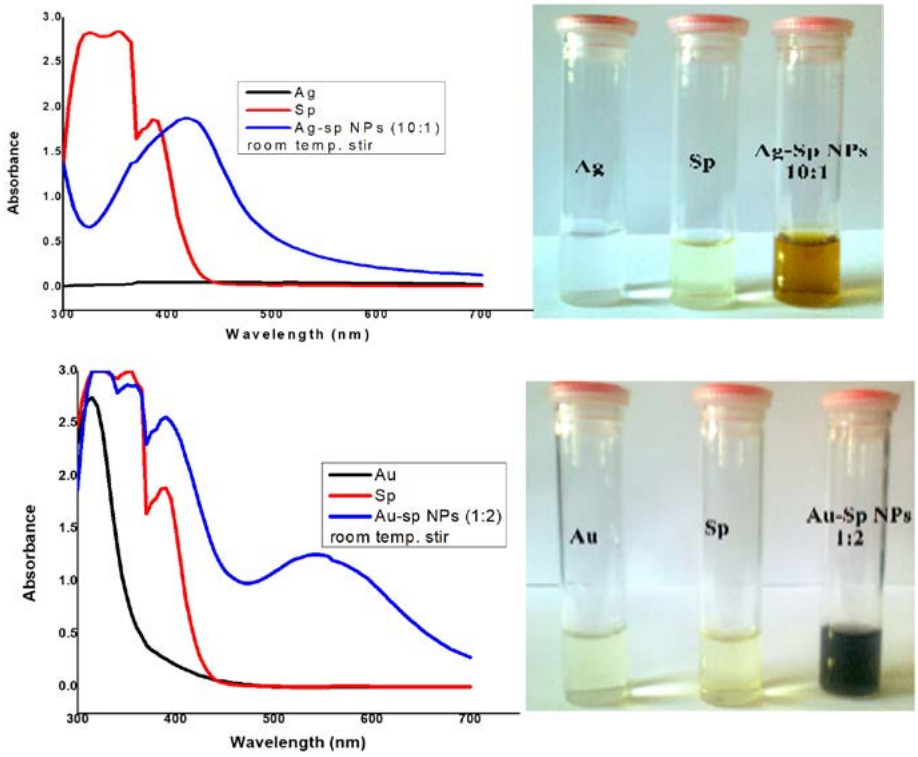

Fig. 2. (a) UV-Vis spectra of optimized Ag-Sp NPs, optical recognition of synthesized silver NPs in inset, (b) UV-Vis spectra of optimized Au-Sp NPs, visual inspection of synthesized gold NPs in inset and the inset photo shows the visual inspection of synthesized gold NPs

For AFM analysis, the Ag-Sp and Au-Sp NPs samples were formed by dissolving thin films in de-ionized water and dispersing on freshly cleaved sheets of mica.

SEM analysis

The morphological analysis of the fabricated Ag-Sp and Au-Sp NPs was performed by SEM (JSM591, JOEL, Japan). The SEM image was recorded at 40,000× magnification operating at 20.00 keV. The presence of Ag and Au in Ag-Sp and Au-Sp NPs was confirmed using the energy dispersive X-ray spectroscopy (EDX, JEOL-JED, 2300). EDX represent the chemical nature of synthesized-NPs.

Anti-bacterial activities of Ag-Sp and Au-Sp NPs

The antibacterial activities were analyzed using well diffusion method with Mueller Hinton agar . Anti-bacterial efficacy of fabricated Ag-Sp and Au-Sp NPs were performed against bacterial strains of *Bacillus subtilis* (ATCC 6633), *Staphylococcus aureus* (ATCC 25925), and *Klebsiella pneumonia* (ATCC 700603) obtained from American Type Culture Collection (ATCC). The culture was developed in triplicates for 72 h at 37°C. The broth standards (0.6 mL) of the species were located in a sterilized *Petri* dish then 20 mL of the sterilized molten Mueller Hinton Broth (MHB) was employed. Streptomycin (2 mg/mL) was utilized as a standard. Inoculation was accomplished for 60 min to facilitate the diffusion of the antibacterial mediator into the medium. Incubation for 24 h at 37°C and the breadths of the zone of inhibition (ZOI) of bacterial development was calculated in the plate in millimeter (mm). After incubation at 37°C for 24 h, the diameter and growth inhibition zones were screened, averaged and the mean values were presented (Abdel-Aziz et al., 2014). The activities were repeated in triplicate.

Statistical analysis

The results collected for microbial activity are displayed as the mean ± standard error of the mean (SEM). The achieved data were assessed to

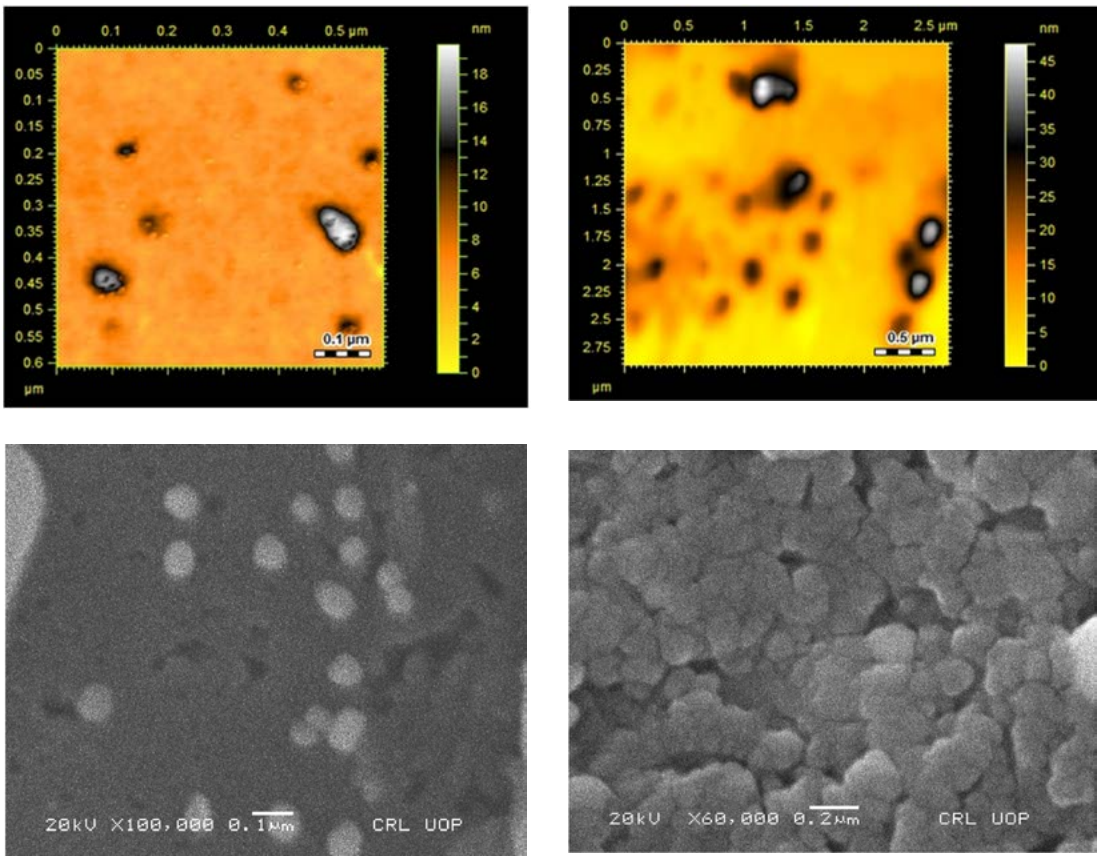

Fig. 3. (a) AFM image of Ag NPs, (b) AFM image of sparfloxacin mediated Au-Sp NPs, (c) SEM images of optimized Ag-Sp NPs, and (d) SEM images of optimized gold NPs

one way analysis of variance (ANOVA). The analysis was done by using Graphpad Prism 5.

RESULTS AND DISCUSSION

UV-Visible analysis

The variation in UV-Vis absorption peaks were considered as the primary indication for the biosynthesis of Ag-Sp NPs and Au-Sp NPs. Absorption maxima of Ag-Sp NPs and Au-Sp NPs were recorded in the range of 300-700 nm as a function of retention time. The presence of particular peaks in the regions of 400-500 nm and 500-600 nm ensured the formation of Ag-Sp NPs and Au-Sp NPs. The sharpest Ag-Sp NPs peak was observed at 10:1 (metal: drug) molar ratio, while for Au-Sp NPs, the sharp peak was at 1:2 (metal: drug) molar ratio as shown in the Fig.s 2 a & b, respectively.

AFM, SEM and EDX analyses

Surface topology and structural features of the formulated Ag-Sp and Au-Sp NPs were investigated by AFM (Fig.s 3 a & b). Micrographs show that the biosynthesized Ag-Sp NPs have a spherical shape and have the sizes in the range of

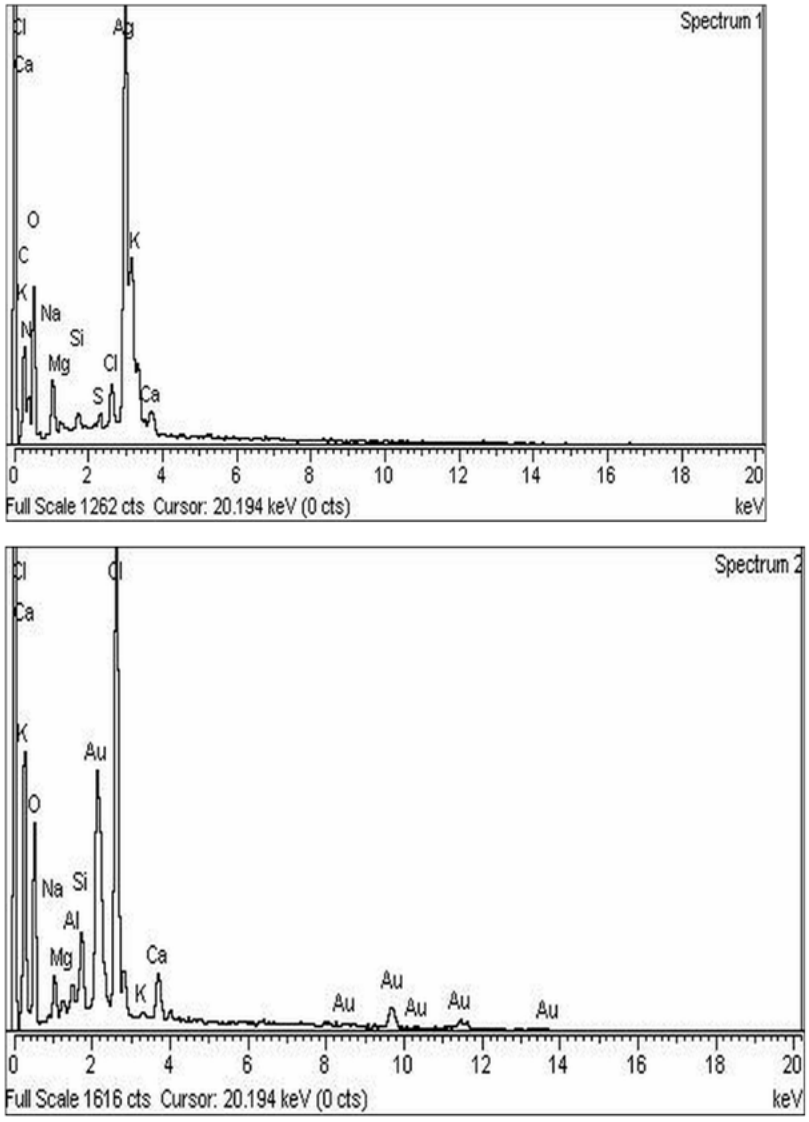

Fig. 4. (a) EDX of synthesized Ag-Sp NPs, (b) EDX of synthesized Au-Sp NPs

40 to 50 nm. The Au NPs have slightly a spherical shape and the mean sizes were in the range of 70 to 80 nm.

The confirmation of surface morphology and the size of Ag-Sp and Au-Sp NPs was also performed by SEM. SEM images indicated spherical Ag-Sp NPs (40-50 nm) with uniform distribution (Fig. 3c). SEM results for Au-Sp NPs were comparable, that further confirming the AFM analyses. The shapes were found to be slightly spherical in the range of 70 to 80 nm as presented in Fig. 3d. EDX illustrated (Fig. 4 a & b) the chemical nature of Ag-Sp and Au-Sp NPs showing signals at an energy of 3 KeV for silver, and 2.12 and 9.71 KeV for gold (Nisar et al., 2015).

FTIR characteristics

FTIR analysis was carried out to determine the presence of functionalities available in the drug (sparfloxacin) before and after stabilizing the Ag-Sp and Au-Sp NPs. Sparfloxacin showed signals for aromatic C-H stretch (2933 cm^{-1}), O-H stretch (2681 cm^{-1}), C=O stretch for ketone (1715 cm^{-1}), secondary N-H stretch (3374 cm^{-1}), and O-H bend of COOH (1446 cm^{-1}), and C-N stretch (1341 cm^{-1}). The band at 3374 cm^{-1} is shifted to 3447 cm^{-1} and broadened in the case of Ag-Sp and Au-Sp NPs. The band at 3354 cm^{-1} is due to N-H stretching of the amine moiety, while the shoulder at 3510 cm^{-1} is due to O-H stretching of carboxylic acid group. In case of Ag-Sp NPs, the FTIR spectra showed a shift in carbonyl peak of carboxylic group from 1715 to 1609 cm^{-1}, and C-N stretching is shifted from 1341 to 1385 cm^{-1}. In case of Au-Sp NPs, a shift from 1715 to 1620 cm^{-1} and for C-N stretch the band is shifted from 1341 to 1390 cm^{-1} were observed (Fig. 5). It was revealed from FTIR results that amine

Table 1. Antibacterial activities of sparfloxacin and its noble metal (Ag/Au) NPs

Bacterial strain	Strain	Sparfloxacin	Ag-Sp NPs	Au-Sp NPs	Streptomycin
		ZOI (mm) at 3 mg/mL			
Staphylococcus aureus	+	30±0.92	24±0.94	24±0.94	30±0.98
Bacillus subtilis	+	30±0.94	22±0.79	22±0.79	30±0.98
Klebsiella pneumonia	-	32±0.92	20±0.98	26±0.92	28±0.75

Well size = 6 mm, Mean ± S.E.M.
STD = Standard

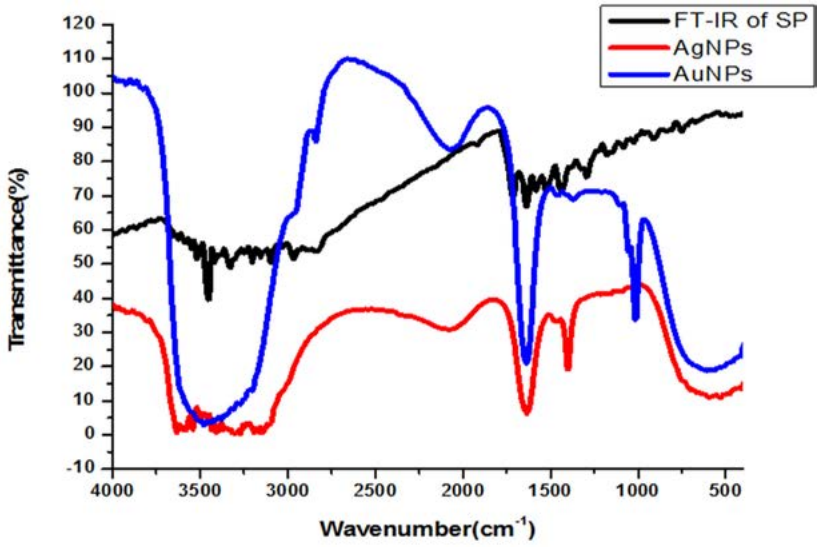

Fig. 5. FTIR spectra of sparfloxacin and its silver and gold NPs

and carboxylate moiety might be responsible for capping and stabilizing of Ag-Sp and Au-Sp NPs (Nisar et al., 2015).

Stability of Ag-Sp and Au-Sp NPs

Fig. 6 (a & b) show the impact of different concentrations of NaCl solution on surface plasmon peak of Ag-Sp and Au-Sp NPs. The results revealed that high concentration of NaCl solution resulted in a decrease in absorbance maxima. The full width at half maximum is increased and thus decreasing the stability of Ag-Sp and Au-Sp NPs. This fast reduction in absorbance of Ag-Sp and Au-Sp NPs containing NaCl is due to the aggregation impact caused by Cl^{-1} ions. As far as long term stability is concerned, Ag-Sp and Au-Sp NPs are more stable in water than in NaCl solution.

The impact of pH on the stability of Ag- and Au-Sp NPs was also conducted. pH values of

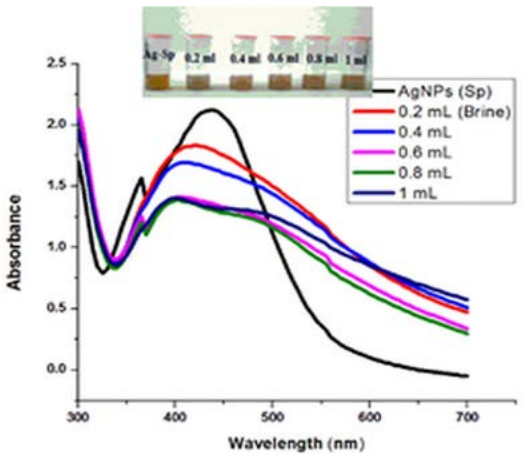

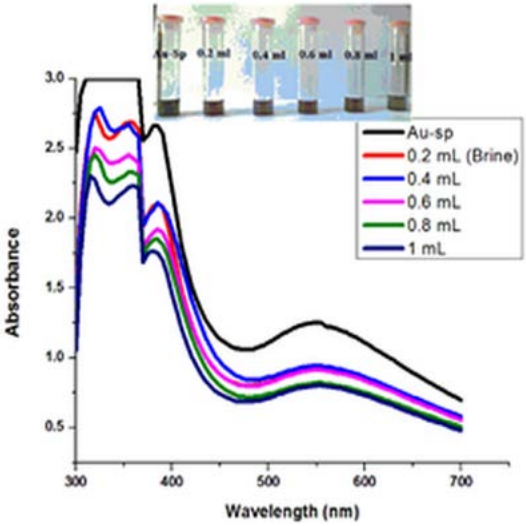

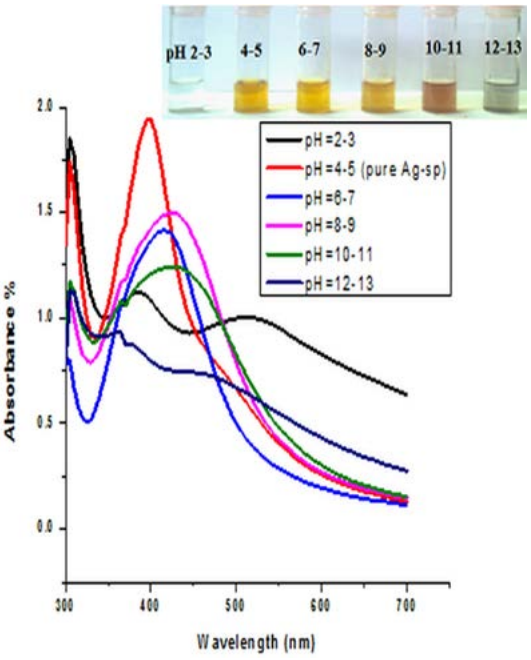

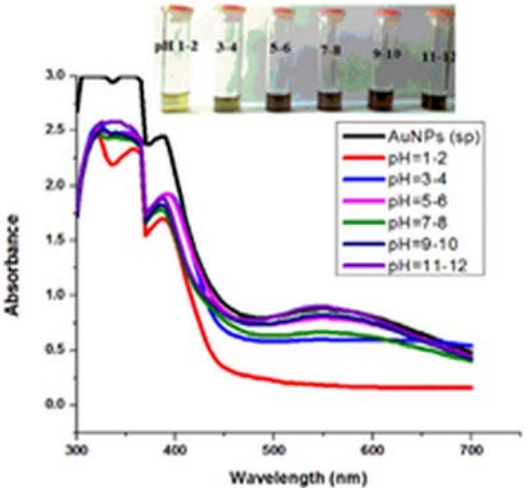

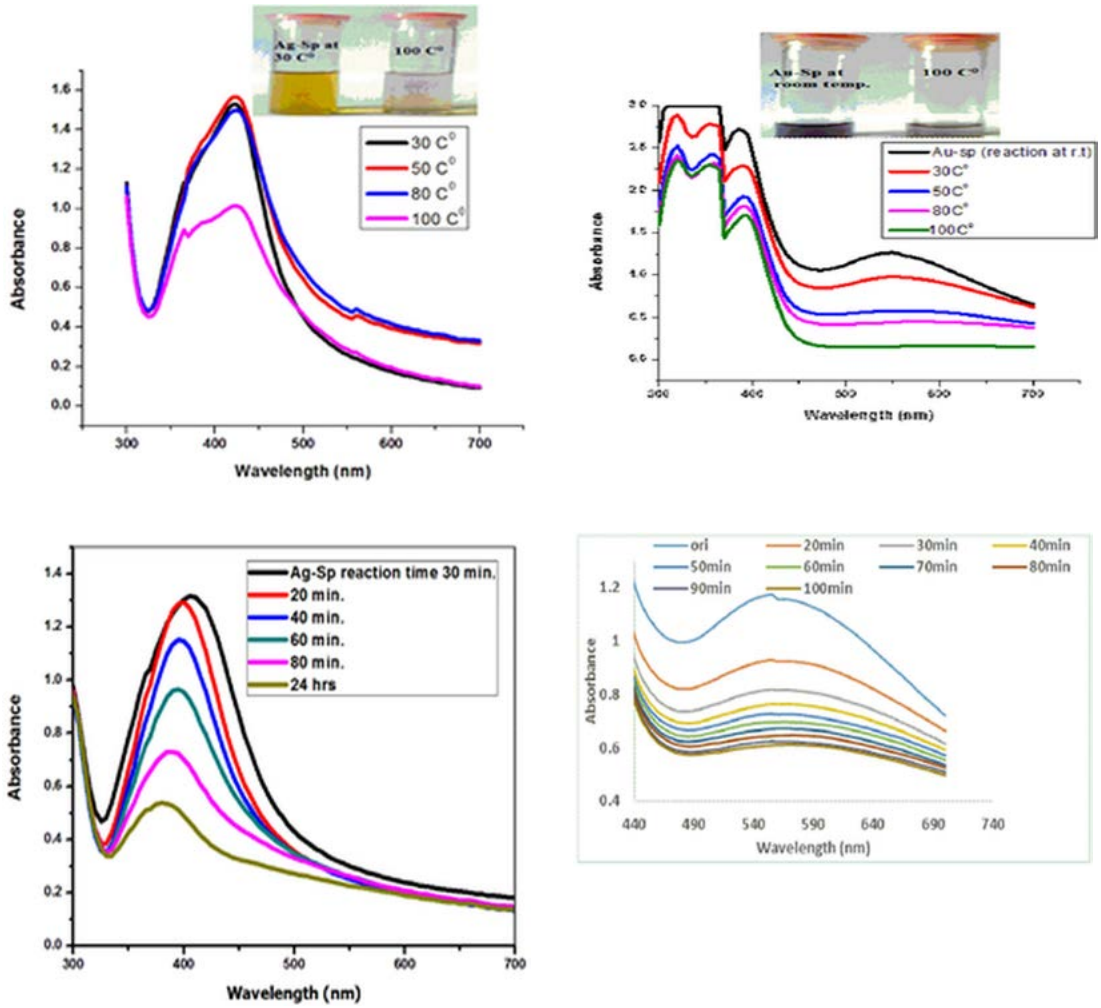

Fig. 6. UV-Vis spectra showing the impact of different volumes of NaCl on stability of Ag-Sp NPs (a) and Au-Sp NPs (b) insets show the change in color of Ag and Au NPs solutions with varying salt (1 M NaCl) concentration correspond to their absorption spectra. Spectral data for the effect of pH on the stability of sparfloxacin-capped Ag NPs (c). Effect of pH on stability of Au-Sp NPs (d). Effect of temperature on the stability of Ag-Sp NPs (Inset: effect of temperature on color of Ag-Sp NPs) (e). Temperature effect on the stability of Au-Sp NPs (Inset: effect of temperature on color of Au-Sp NPs) (f). Effect of reaction time on stability of Ag-Sp NPs (g), and Au-Sp NPs (h).

3 mL solutions of the freshly prepared NPs were 4.49 (Ag-Sp NPs), and 9.66 (Au-Sp NPs). pH of 1-7 was adjusted using 1M HCl solution while that of 7-12 was adjusted using 1M NaOH solution. UV-Vis spectra of resulting solution was screened after 24 h (Fig. 6 c & d).

Temperature is an important factor that affects the stability and properties of Ag-Sp NPs and Au-Sp NPs. Ag-Sp NPs were stable at broad range of temperatures (Nisar et al., 2016) (Fig. 6e). Surface plasmon resonance (SPR) bands up to 100°C indicated a decrease in intensity with a blue shift from the original band that is due to NPs degradation with decrease in particle size. Au-Sp NPs exhibited also less stability by increasing the temperature to 100°C. Temperature also affect the color of Au-Sp NPs, wherein the color changes from pink-purple to colorless, indicating

the aggregation of Au-Sp NPs with the increase in temperature (Khan et al., 2019) (Fig. 6f).

In order to optimize the time needed for the completion of reaction, the impact of time on the reaction was investigated using UV-Vis for colloidal suspension of Ag-Sp and Au-Sp NPs, whereas the reaction was screened from zero to 80 min at 10 min time interval. The absorption peak rapidly increased with the increase in reaction time from 10 to 30 min because of the continuous formulation of Ag-Sp NPs and Au-Sp NPs. It was noted that an optimum time is needed for the completion of reaction because of the instability of Ag-Sp NPs. The optimum time needed for the completion of reaction was 30 min for Ag-Sp NPs while for Au-Sp NPs was 5 min (Fig. 6 g & h).

Anti-bacterial properties

Ag-Sp and Au-Sp NPs anti-bacterial activities were screened against bacterial strains including *Staphylococcus aureus, Bacillus subtilis*, and *Klebsiella pneumonia*, by agar well diffusion method (Table 1). The inhibition zones indicated that Ag-Sp NPs and Au-Sp NPs are active antibacterial agents against a range of bacteria. At a concentration of 3 mg/mL, Ag-Sp NPs and Au-Sp NPs revealed significant anti-bacterial activity against tested stains, showing a ZOI ranging from 20±0.98 to 24±0.94 mm (Ag-Sp NPs), and 22±0.79 to 26±0.92 mm (Au-Sp NPs). The results were comparable with sparfloxacin (30±0.92-32±0.94 mm) and the standard streptomycin (28±0.75-30±0.98 mm).

Staphylococcus aureus is a Gram-positive bacterium that develops resistant against antibiotics such as tetracycline, penicillin, semisynthetic penicillin, and aminoglycosides. The reason for this resistance could be the overuse of antibiotic (Reddy et al. 2012; Mittal et al., 2016). *Bacillus subtilis* is a Gram-positive bacterium, found in the gastrointestinal tract of humans and ruminants and as well as in the soils. There is limited information on their resistance to antibiotics. Many *Bacillus subtilis* were sensitive to vancomycin (4 mg/L), tetracycline (8 mg/L), and gentamicin (4 mg/L), but resistant to streptomycin. The sensitivity to chloramphenicol, clindamycin, and kanamycin was a species specific (Adimpong et al., 2012). *Klebsiella pneumoniae* is considered the most encountered carbapenemase-producing *Enterobacteriaceae* (Won et al., 2011). Increasing the antimicrobial drug resistance, including carbapenem-resistant *K. pneumoniae* (CRKP), depend on the substantial increases in illness (Won et al., 2011). Few antimicrobial therapies are exist for CRKP infections (Sanchez et al., 2013).

CONCLUSION

A rapid, facile and time effective protocol, to formulate noble metal (Ag/Au) NPs stabilized with sparfloxacin, was introduced. Synthesized-NPs had sizes in the range of 40-45 nm (Ag) and 70-80 nm (Au), respectively. The results showed the potential to produce stable noble metal (Ag/Au) NPs stabilized with sparfloxacin confirmed by different methods such as FTIR, UV-vis spectroscopy, AFM and SEM. Stabilities of Ag-Sp NPs and Au-Sp NPs were tested under different conditions including temperature, salt solution, pH, and time. The results revealed that both Ag-Sp NPs and Au-Sp NPs are sable. EDX analysis confirmed the inorganic structure of the biosynthesized Ag-Sp NPs and Au-Sp NPs. The synthesized Ag-Sp NPs and Au-Sp NPs are freely water soluble. Analysis showed that amine and carboxylate moiety might be a cause of NPs capping. Moreover, Ag-Sp and Au-Sp NPs exhibited good antibacterial potential against Gram-negative and Gram-positive bacteria.

ACKNOWLEDGMENTS

Shujaat Ali Khan is grateful to the Higher Education Commission of Pakistan for financial support.

CONFLICT OF INTEREST

The authors declare that there is no conflict of interest.

AUTHORS' CONTRIBUTION

MN, SAK, MG, AR, SZ drafted the manuscript, compiled information from the literature, and designed the Fig.s and tables. MN, SAK, MG, AR, SZ drafted the manuscript and gathered information from the literature. MFR reviewed the manuscript.

FUNDING

Authors are grateful to the Higher Education Commission of Pakistan for financial support under the indigenous PhD program.

ETHICS STATEMENT

This article does not contain any studies with human participants or animals performed by any of the authors.

DATA AVAILABILITY

All datasets generated or analyzed during this study are included in the manuscript.

REFERENCES

1. Abdel-Aziz MS, Shaheen MS, El-Nekeety AA, Abdel-Wahhab MA. Antioxidant and antibacterial activity of silver nanoparticles biosynthesized using *Chenopodium murale* leaf extract. *Journal of Saudi Chemical Society*. 2014;18(4):356-363. doi: 10.1016/j.jscs.2013.09.011
2. Abdelghany TM, Al-Rajhi AMH, Al Abboud MA, et al. Resent advances in green synthesis of silver nanoparticles and their applications: About future directions. A Review. *BioNanoSci.* 2018;8(1):5-16. doi: 10.1007/s12668-017-0413-3
3. Adimpong DB, Sorensen KI, Thorsen L, et al. Antimicrobial susceptibility of *Bacillus* strains isolated from primary starters for African traditional bread production and characterization of the bacitracin operon and bacitracin biosynthesis. *Appl Environ Microbiol*. 2012;78(22):7903-7914. doi: 10.1128/AEM.00730-12.
4. Al-Shmgani HSA, Mohammed WH, Sulaiman GM, Saadoon AH. Biosynthesis of silver nanoparticles from *Catharanthus roseus* leaf extract and assessing their antioxidant, antimicrobial and wound healing activities. *Artif Cells Nanomed Biotechnol*. 2017;45(6):1234-1240.doi: 10.1080/21691401.2016.1220950
5. Alvarez MM, Khoury JT, Schaaff TG, Shafigullin MN, Vezmar I, Whetten RL. Optical absorption spectra of nanocrystal gold molecules. *J Phys Chem*. 1997;101(19):3706-3712. doi: 10.1021/jp962922n
6. Andriole VT. The Quinolones, third ed., Academic Press, San Diego. 2000. doi: 10.1016/B978-012059517-4/50017-9
7. Arvizo RR, Bhattacharyya S, Kudgus RA, Giri K, Bhattacharya R, Mukherjee P. Intrinsic therapeutic applications of noble metal nanoparticles: Past, present and future. *Chemical Society Reviews*. 2012;41(7):2943-70. doi: 10.1039/c2cs15355f
8. Basavegowda N, Idhayadulla A, Lee YR. Preparation of Au Ag nanoparticles using *Artemisia annua* and their *in vetro* antibacterial and tyrosinase inhibitory activities. *Materials Science and Engineering: C*. 2014;43(1):58-64. doi: 10.1016/j.msec.2014.06.043
9. Cao G. Nanostructures and Nanomaterials. Imperial C ollege Press, London. 2004.
10. Chandra H, Patel D, Kumari P, Jangwan JS, Yadav S. Pyto-mediated synthesis of zinc oxide nanoparticles of *Berberis aristata*:Characterization, antioxidant activity and antibacterial activity with special reference to urinary tract pathogens. *Materials Science and Engineering: C.* 2019;102:212-220. doi: 10.1016/j.msec.2019.04.035
11. Ghaffari-Moghaddam M, R Hadi-Dabanlou. Plant mediated green synthesis and antibacterial activity of silver nanoparticles using *Crataegus douglasii* fruit extract. *Journal of Industrial and Engineering Chemistry*. 2014;20(2):739-744. doi: 10.1016/j.jiec.2013.09.005
12. Hooper DC, Rubinstein E. Quinolone Antimicrobial Agents, third ed., ASM Press, Washington, DC. 2003. doi: 10.1128/9781555817817
13. Huang WC, Tsai PJ, Chen YC. Multifunctional Fe3O4@Au nano eggs as photothermal agents for selective killing of nosocomial and antibiotic-resistant bacteria. *Nanomedicine*. 2007;2:777.
14. Hyllested JE, Palanco ME, Hagen N, Mogensen KB, Kneipp K. Green preparation and spectroscopic characterization of plasmonic silver nanoparticles using fruits as reducing agents. *Beilstein J Nanotechnol*. 2015;6:293-9. doi: 10.3762/bjnano.6.27
15. Ismail RA, Sulaiman GM, Mohsin MH, Saadoon AH. Preparation of Silver Iodide Nanoparticles using Laser Ablation in liquid for Antibacterial Applications. *IET Nanobiotechnology.* 2018;12(6):781-786. doi: 10.1049/iet-nbt.2017.0231
16. Johnson alias Antonysamy M, Santhanam A, Thangaiah S, Narayanan J. Green synthesis of silver nanoparticles using *Cyathea nilgirensis* Holttum and their cytotoxic and phytotoxic potentials. *Particulate Science and Technology*. 2018;36(5):578-585. doi: 10.1080/02726351.2016.1278292
17. Keshavamurthy M, Srinath BS, Rai VR. Phytochemicals-mediated green synthesis of gold nanoparticles using *Pterocarpus santalinus* L. (Red Sanders) bark extract and their antimicrobial properties. *Particulate Science and Technology.* 2018;36(7):785-790. doi: 10.1080/02726351.2017.1302533
18. Khan I, Saeed K, Khan I. Nanoparticles: Properties, applications and toxicities. *Arabian Journal of Chemistry*. 2019;12(7):908-931. doi: 10.1016/j.arabjc.2017.05.011
19. King DE, Malone R, Lilley SH. New classification and update on the quinolone antibiotics. *Am Fam Physician*. 2000;61:2741-2748.
20. Majumdar R, Bag BG, Ghosh P. *Mimusops elengi* bark extract mediated green synthesis of gold nanoparticles and study of its catalytic activity. *Appl Nanosci*. 2015;6(4):521-528. doi: 10.1007/s13204-015-0454-2
21. Maniraj A, Kannan M, Rajrathinam K, Vivekanandhan S, Muthuramkumar S. Green synthesis of silver nanoparticles and their effective utilization in fabricating functional surface for antibacterial activity against multi-drug resistant *Proteus mirabilis*. *Journal of Cluster Science*. 2019;30:1403-1414. doi: 10.1007/s10876-019-01582-z
22. Marulasiddeshwara MB, Dakshyani SS, Kumar MNS, Chethana R, Kumar PR, Devaraja S. Facile-one pot-green synthesis, antibacterial, antifungal, antioxidant and antiplatelet activities of lignin capped silver nanoparticles: a promising therapeutic agent. *Material Science and Engineering C*. 2017;81:182-190. doi: 10.1016/j.msec.2017.07.054
23. Metuku RP, Pabba S, Burra S, Bindu SVSSSLM, Gudikandula K, Singara CMA. Biosynthesis of silver

nanoparticles from *Schizophyllum radiatum* HE 863742.1: their characterization and antimicrobial activity. *3 Biotech*. 2014;4:227-234. doi: 10.1007/s13205-013-0138-0

24. Mikhailov OV, Mikhailova EO. Elemental silver nanoparticles: Biosynthesis and Bio Applications. *Materials*. 2019;12(19):3177. doi: 10.3390/ma12193177
25. Mitscher LA. Bacterial topoisomerase inhibitors: quinolone and pyridone antibacterial agents. *Chemical Reviews.* 2005;105(2):559-592. doi: 10.1021/cr030101q
26. Mittal J, Singh A, Batra A, Sharma MM. Synthesis and characterization of silver nanoparticles and their antimicrobial efficacy. *Particulate Science and Technology*. 2017;35(3):338-345. doi: 10.1080/02726351.2016.1158757
27. Nath SS, Chakdar D, Gope G, Avasthi DK. Characterizations of CdS and ZnS quantum dots prepared by chemical method on SBR latex. *J Nanotechnol.* 2008;4:1-6.
28. Nisar M, Khan SA, Qayum M, et al. Robust synthesis of ciprofloxacin-capped metallic nanoparticles and their urease inhibitory assay. *Molecules*. 2016;21(4):411. doi: 10.3390/molecules21040411
29. Nisar M, Khan SA, Shah MR, et al. Moxifloxacin-capped noble metal nanoparticles as potential urease inhibitors. *New Journal Chemistry*. 2015. doi: 10.1039/C5NJ01571E
30. Pissuwan D, Valenzuela SM, Miller CM, Cortie MB. A golden bullet? Selective targeting of T*oxoplasma gondii* tachyzoites using antibody-functionalized gold nanorods. *Nano Letters.* 2007;7(12):3808-3812. doi: 10.1021/nl072377+
31. Rao CNR, Kulkarni GU, Thomas PJ, Edwards PP. Metal nanoparticles and their assemblies. *Chemical Society Reviews*. 2000;29:27-35. doi: 10.1039/a904518j
32. Reddy CM, Thati V, Shivannavar CT, Gaddad SM. Vancomycin resistance among methicillin resistant *Staphylococcus aureus* isolates in Rayalaseema region Andhra Pradesh, South India. *World Journal of Scientific Technology*. 2012;2:6-8.
33. Reed M A, Lee T. Molecular Nanoelectronics, American Scientific Publishers, Valencia, CA. 2003.
34. Rizwan M, Amin S, Malikovna BK, et al. Green Synthesis and Antimicrobial Potential of Silver Nanoparticles with *Boerhavia procumbens* Extract. *J Pure Appl Microbiol.* 2020;14(2):1437-1451. doi: 10.22207/JPAM.14.2.42.
35. Sanchez GV, Master RN, Clark RB, Fyyaz M, Duvvuri P, Ekta G. *Klebsiella pneumoniae* Antimicrobial Drug Resistance, United States, 1998-2010. *Emerg Infect Dis*. 2013;19(1):133-136. doi: 10.3201/eid1901.120310.
36. Singh A, Jain D, Upadhyay MK, Khandelwal N, Verma HN. Green synthesis of silver nanoparticles using Argemone Mexicana leaf extract and evaluation of their antimicrobial activities. *Digest Journal of Nanomaterials and Biostructures*. 2011;5(2):483-439.
37. Singh A, Sharma MM, Batra A. Synthesis of gold nanoparticles using chick pea leaf extract using green chemistry. *Journal of Optoelectronic and Biomedical Materials*. 2013;5(2):27-32.
38. Stein GE. Pharmacokinetics and pharmacodynamics of newer fluoroquinolones. *Clin Infect Dis.* 1996;23(Suppl 1:S19-S24. doi: 10.1093/clinids/23.Supplement_1.S19
39. Sulaiman GM, Ali EH, Jabbar II, Saleem AH. Synthesis, characterization, antibacterial and cytotoxic effects of silver nanoparticles. *Digest Journal of Nanomaterials and Biostructures*. 2014;9:787-796.
40. Sulaiman GM, Hussien HT, Saleem MMNM. Biosynthesis of silver nanoparticles synthesized by *Aspergillus flavus* and their antioxidant,antimicrobial and cytotoxicity properties. *Bulletin of Materials Science*. 2015;38(3):639-644. doi: 10.1007/s12034-015-0905-0
41. Sulaiman GM, Waheeb HM, Jabir MS, Khazaal SH, Dewir YH, Naidoo DY. Biocompatible, Anti-Cancer, Anti-Inflammatory and Phagocytosis Inducer Model. *Sci Rep*. 2020;10: 1-16. doi:
42. Taha ZK, Hawar SN, Sulaiman GM. Extracellular biosynthesis of silver nanoparticles from *Penicillium italicum* and its antioxidant, antimicrobial and cytotoxicity activities. *Biotechnol Lett*. 2019;41:899-914. doi: 10.1007/s10529-019-02699-x
43. Turel I. The interactions of metal ions with quinolone antibacterial agents. *Coordination Chemistry Reviews*. 2002;232(1-2):27-47. doi: 10.1016/S0010-8545(02)00027-9
44. Waheeb HM, Sulaiman GM, Jabir M. Effect of hesperidin conjugated with golden nanoparticles on phagocytic activity: *In vitro* study. *AIP Conference Proceedings*. 2020;2213(1):020217. doi: 10.1063/5.0000159
45. Wang X, Zhuang J, Peng Q, Li Y. A general strategy for nanocrystal synthesis. Nature. 2005;437:121-124. doi: 10.1038/nature03968
46. Won SY, Munoz-Price LS, et al. Emergence and rapid regional spread of *Klebsiella pneumoniae* carbapenemase-producing *Enterobacteriaceae*. *Clin Infect Dis*. 2011;53(6):532-540. doi: 10.1093/cid/cir482
47. Xiangqian L, Xu H, Chen ZS, Chen G. Biosynthesis of nanoparticles by microorganisms and their applications. *Journal of Nanomaterials*. 2011;2011:1-16. doi: 10.1155/2011/270974
48. You C, Han C, Wang X, et al. The progress of silver nanoparticles in the antibacterial mechanism, clinical application and cytotoxicity. *Mol Bio Rep*. 2012;39:9193-9201. doi: 10.1007/s11033-012-1792-8
49. Zharov VP, Mercer KE, Galitovskaya EN, Smeltzery MS. Photothermal nanotherapeutics and nano diagnostics for selective killing of bacteria targeted with gold nanoparticles. *Biophys J.* 2006;90(2):619-627. doi: 10.1529/biophysj.105.061895